



Efficacy of ^{68}Ga -PSMA-11 PET/CT with biparametric MRI in diagnosing prostate cancer and predicting risk stratification: a comparative study

Yi Nuo^{1#}, Aimei Li^{2#}, Lulu Yang³, Hailin Xue¹, Feng Wang⁴, Liwei Wang¹

¹Department of Radiology, Nanjing First Hospital, Nanjing Medical University, Nanjing, China; ²Department of Nuclear Medicine, Nanjing Drum Tower Hospital, The Affiliated Hospital of Nanjing University Medical School, Nanjing, China; ³Department of Pathology, Nanjing First Hospital, Nanjing Medical University, Nanjing, China; ⁴Department of Nuclear Medicine, Nanjing First Hospital, Nanjing Medical University, Nanjing, China

Contributions: (I) Conception and design: Y Nuo, L Wang; (II) Administrative support: L Wang; (III) Provision of study materials or patients: L Yang, H Xue, F Wang; (IV) Collection and assembly of data: Y Nuo, L Wang; (V) Data analysis and interpretation: Y Nuo, A Li, L Wang; (VI) Manuscript writing: All authors; (VII) Final approval of manuscript: All authors.

[#]These authors contributed equally to this work.

Correspondence to: Liwei Wang. Department of Radiology, Nanjing First Hospital, Nanjing Medical University, 68th Changle Road, Qinhuai District, Nanjing 210006, China. Email: wei2030@hotmail.com; Feng Wang. Department of Nuclear Medicine, Nanjing First Hospital, Nanjing Medical University, 68th Changle Road, Qinhuai District, Nanjing 210006, China. Email: fengwangcn@hotmail.com.

Background: This retrospective study aimed to investigate the efficacy of the combined application of biparametric magnetic resonance imaging (bpMRI) and ^{68}Ga -PSMA-11 positron emission computed tomography/computed tomography (bpMRI/PET) in the qualitative diagnosis of intermediate- to high-risk prostate cancer (PCa).

Methods: The 105 patients with suspected PCa included in the study underwent bpMRI and PET/CT. BpMRI examinations included conventional sequences and diffusion-weighted imaging (DWI) sequences. Major lesions were qualitatively diagnosed according to the Prostate Imaging Reporting and Data System (PI-RADS). A PET/CT scan was started 60 min after intravenous ^{68}Ga -PSMA-11 injection. The area with the highest radioactivity on PET/CT images was defined as the major lesion, and the maximum standard uptake value (SUV_{max}) was measured. All cases were confirmed by biopsy and pathology. Receiver operating characteristic curve (ROC) analysis was performed on the data to calculate sensitivity, specificity, and the Youden index.

Results: Of the 105 patients, 68 patients were diagnosed with PCa, and 37 patients had benign prostatic lesions. With a PI-RADS score ≥ 3 as the diagnostic threshold, the accuracy of bpMRI in identifying benign and malignant prostate lesions was similar to that of PET/CT (SUV_{max} threshold ≥ 10.9), and the Youden indices were 0.60 and 0.64, respectively. The sensitivity and specificity of bpMRI in the differential diagnosis of intermediate- to high-risk PCa versus low-risk PCa or benign lesions were 63% and 88%, respectively, and the Youden index was 0.51. With an $\text{SUV}_{\text{max}} \geq 12.9$ as the diagnostic threshold, the sensitivity and specificity of PET/CT in the differential diagnosis of intermediate- to high-risk PCa versus low-risk PCa or benign lesions were 74% and 94%, respectively, and the Youden index was 0.68. The sensitivity and specificity of bpMRI/PET in diagnosing PCa were 94% and 81%, respectively, and the Youden index was 0.75. The sensitivity and specificity of bpMRI/PET in the differential diagnosis of intermediate- to high-risk PCa versus low-risk PCa or benign lesions were 80% and 88%, respectively, and the Youden index was 0.68.

Conclusions: The combined application of bpMRI and PET improves the accuracy of the qualitative diagnosis of prostate lesions, and its diagnostic efficacy for risk stratification in patients with intermediate- to

high-risk PCa is similar to that of PET/CT and higher than that of bpMRI alone.

Keywords: Prostate cancer (PCa); magnetic resonance imaging (MRI); positron emission computed tomography (PET); prostate-specific membrane antigen (PSMA)

Submitted Jan 23, 2021. Accepted for publication May 26, 2021.

doi: 10.21037/qims-21-80

View this article at: <https://dx.doi.org/10.21037/qims-21-80>

Introduction

Prostate cancer (PCa) is the second most common malignant tumour according to mortality in elderly men. The biological behaviour of high-risk PCa can seriously damage patients' health, and early diagnosis and treatment can improve the quality of life and prognosis of these patients (1,2). Multiparameter magnetic resonance imaging (mpMRI) can produce images with high spatial resolution, and its imaging features are highly correlated with histopathological characteristics. MpMRI is commonly used to detect high-risk lesions and ignore low-risk lesions and is a reliable noninvasive method for diagnosing and staging PCa. Compared with systemic puncture biopsy, mpMRI has higher sensitivity and negative predictive value (3-5). At least three mpMRI sequences are needed to diagnose PCa: T2-weighted imaging (T2WI), dynamic contrast-enhanced imaging (DCEI), and diffusion-weighted imaging (DWI). In the second edition of the Prostate Imaging Reporting and Data System (PI-RADS), DCEI plays a minor role, but DWI and its derived apparent diffusion coefficient (ADC) maps have become the main diagnostic parameters (6,7).

In recent years, many studies have shown that the diagnostic efficacy of biparametric MRI (bpMRI), including only T2WI and DWI, is basically the same as that of mpMRI, and bpMRI has been able to meet the diagnostic needs of routine examinations (8,9). A review published by Alabousi *et al.* (10) showed that the sensitivity and specificity of mpMRI are 86% and 73%, respectively, while the sensitivity and specificity of bpMRI are 90% and 70%, respectively. Diagnostic efficacy did not significantly differ between bpMRI and mpMRI. However, the specificity of MRI in diagnosing PCa is not sufficiently high. More than one-fourth of patients are overdiagnosed, whereas 10% of patients with certain evidence of PCa are misdiagnosed. A diagnostic technique with higher specificity is needed to compensate for this shortcoming.

Prostate-specific membrane antigen (PSMA) is an inherent transmembrane protein located in the membrane

of the prostate epithelium. Compared with that in benign prostate tissue, PSMA is overexpressed in more than 90% of PCa cells, and higher PSMA expression indicates a higher grade of malignancy (11,12). The positron emission tomography/computed tomography (PET/CT) tracer ^{68}Ga -PSMA-11 composed of a PSMA-targeting ligand is an effective agent for targeted diagnosis and treatment of PCa and is superior to any other PET radioligand (13,14). ^{68}Ga -PSMA-11 PET/CT examination has high sensitivity and specificity for displaying primary, recurrent, and metastatic PCa lesions and can identify most benign lesions, such as benign prostatic hyperplasia (BPH) and prostatitis. Compared to MRI, this modality can better display recurrent and metastatic lesions (15).

BpMRI is a cost-effective advanced technique without possible side effects from contrast agent injection and is more easily accepted by patients. PET/CT examination using PCa-specific tracers can provide more molecular information, but the economic cost is relatively high. Preoperative PET/CT for patients with suspected PCa on MRI is necessary and can improve qualitative diagnosis and staging. The purpose of this study was to investigate the efficacy of the combined application of bpMRI and PET/CT (bpMRI/PET) in the qualitative diagnosis of intermediate- to high-risk PCa.

Methods

Patients

This is a retrospective study. From January 2017 to May 2020, a total of 493 consecutive patients underwent PET/CT examinations in our hospital, 230 of whom underwent bpMRI. The reasons and symptoms prompting patients to undergo the examinations included dysuria, haematuria, elevated prostate-specific antigen (PSA), and routine physical examination. Before the PET/CT scans, all patients underwent ultrasound or PSA screening, and then patients with elevated PSA or suspicious lesions detected

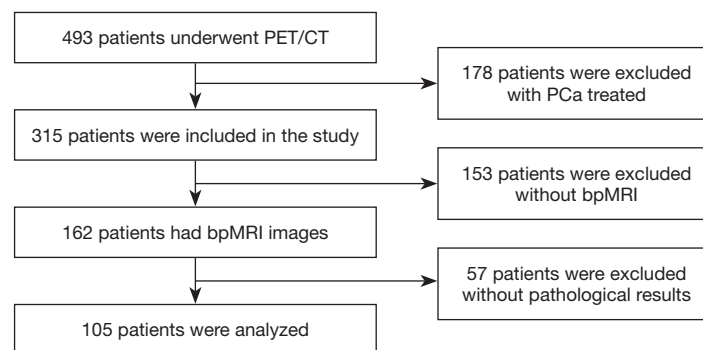


Figure 1 The flow chart of eligible patient inclusion. PCa, prostate cancer.

by ultrasound underwent PET/CT, MRI, or biopsy. The inclusion criteria were (I) digital rectal examination or transrectal ultrasound revealing suspicious nodules of the prostate; (II) an elevated PSA level and the need for PCa screening or differential diagnosis; (III) BpMRI, PET/CT, and puncture biopsy performed within 30 days; (IV) successful imaging examination and a definitive pathological diagnosis. The exclusion criteria were (I) recurrent PCa; (II) an interval between the three examinations greater than 30 days; (III) a diagnosis of PCa with a history of treatment; (IV) no definitive pathological diagnosis. A total of 105 patients were included and underwent both PET/CT and bpMRI before prostate biopsies in the study (*Figure 1*). The mean age of the patients was 68.37 ± 10.21 years (range: 43 to 89 years), and the PSA level ranged from 3.45 to 1,000 ng/mL. The study was conducted in accordance with the Declaration of Helsinki (as revised in 2013). The study was approved by ethics board of KY20171208-03 and individual consent for this retrospective analysis was waived. The diagnoses of all patients were confirmed by surgery or pathological analysis of a biopsy specimen.

MRI techniques

A Philips high-field-strength double-gradient superconducting MRI scanner (Intera Achieva 3.0T TX, Philips, Netherlands) was used for the examination. The phased array coil was placed on the abdomen of the patient before the examination. The centre of the coil was approximately at the level of the pubic symphysis. The MRI acquisition sequence included axial T1WI [repetition time (TR) 400 ms, echo time (TE) 10 ms, slice thickness 4.0 mm], axial, sagittal, and coronal T2WI (TR 3,000 ms, TE 100 ms, slice thickness 3.0 mm), fat suppressed T2WI (TR 2,800 ms, TE 100 ms, slice thickness 3.0 mm), and axial DWI

(TR 6,000 ms, TE 2,000 ms, slice thickness 4.0 mm, $b=0/50/1,500$ s/mm²).

PET/CT examination

PSMA-11 was purchased from ABX (Germany). We used an automated labelling module (ITG, Germany) to synthesize ⁶⁸Ga-PSMA-11. The agent was prepared in accordance with Class IV laboratory standards, and the radiochemical purity was 93–99%. The net-injected doses were calculated by subtracting the residual syringe activity. Patients were weighed on the day of the exam. Standard uptake value (SUV) calculations were performed utilizing the plain body weight. ⁶⁸Ga-PSMA-11 was administered intravenously. The patients were instructed to drink plenty of water and to urinate before the scan. At 45 and 60 min after injection, nonenhanced CT scans (130 kV, 80 mA, slice thickness 3 mm) and PET/CT (United Imaging, uMI780, China) were performed, respectively. PET acquisition included four beds at 3 min/per bed. Daily quality assurance/quality control measures were implemented for the scanners. After CT data correction, iterative reconstruction was performed. PET and CT images were fused at a workstation to obtain axial, coronal, and sagittal images.

Biopsy procedure

All patients underwent transrectal ultrasound-guided biopsy within 30 days of completing the MRI and PET examinations. The prostate is divided into three parts from top to bottom: basal, body, and apical. Each part is divided into left and right zones. The left and right zones in the basal and body parts are subdivided into medial and lateral aspects. The prostate includes 10 zones in total. Puncture biopsy was performed in each zone. After the systematic

Table 1 Rating program of PI-RADS

DWI	Peripheral zone		Central gland zone		
	T2WI	PI-RADS	T2WI	DWI	PI-RADS
1	Any	1	1	Any	1
2	Any	2	2	Any	2
3	≤3	3	3	≤4	3
3	≥4	4	3	5	4
4	Any	4	4	Any	4
5	Any	5	5	Any	5

T2WI, T2 weighted imaging; DWI, diffusion weighted imaging; PI-RADS, prostate imaging-reporting and data system.

biopsy, an additional targeted biopsy was performed in the corresponding position of the region of interest (ROI) of bpMRI and PET/CT to ensure the accuracy of pathological results. The physician who performed the biopsy recorded the puncture site in detail. The biopsy specimens were diagnosed by pathologists, and the Gleason score (GS) was determined. Malignant lesions with a GS =6 were defined as low-risk PCa, and malignant lesions with a GS ≥7 were defined as moderate- to high-risk PCa (16).

Image analysis

Four experienced readers—two radiologists specialising in MRI and two radiologists specialising in PET—who were blinded to the pathology and clinical results worked together to mark the locations of suspected lesions separately on the MRI and PET/CT images for image analysis and puncture biopsy guidance. They measured the average ADC values and the maximum SUV (SUV_{max}) before establishing a differential diagnosis. A suspected lesion is denoted by a low-signal intensity area at the central zone on T2WI and a high-signal intensity area at the peripheral zone on DWI or bpMRI or an area with increased tracer uptake on PET. The area with the highest radioactivity on PET/CT images was defined as the major lesion, and the SUV_{max} was measured. When the suspicious lesion locations from the two methods were not consistent, a senior MRI physician and a senior PET/CT physician discussed the final decision. To ensure accurate measurements, lines should be drawn along the boundaries of lesions, including the whole focus as far as possible, thus ensuring that the area with the highest radioactivity is included when drawing the ROI. According to the second edition of the 2015 PI-RADS, two radiologists specialising in MRI performed a qualitative

diagnosis and T staging according to the bpMRI study (T2WI + DWI). The PI-RADS categories were divided into five grades. The sequences for grading included axial and sagittal T2WI and axial DWI (including the corresponding ADC map). Lesions (with a score of 3) in the peripheral zone of the prostate on DWI were scored on T2WI instead of DCEI. The specific scoring criteria are shown in *Table 1*. Two radiologists specialising in PET analysed the PET/CT images, obtained the SUV_{max} of the suspected lesion as the diagnostic basis, and performed T staging. T staging included prostate adenocarcinoma extracapsular invasion (EPE), seminal vesicle gland invasion (SVI), and pelvic lymph node metastasis (PLNM).

Statistical analysis

The diagnostic efficacy of the imaging study in each patient was evaluated based on histopathology. The quantitative data were first tested for normality. Data with a normal distribution are expressed as the mean ± standard deviation ($\bar{x} \pm s$) and were compared using the independent-sample *t* test. Data without a normal distribution are expressed as the median (upper quartile, lower quartile) [M (P25, P75)] and were compared using the Mann-Whitney U test. Cohen's κ value was used to evaluate the consistency of the diagnosis of PCa between the radiologists who reviewed PET/CT or MRI images. The sensitivity and specificity of the two imaging methods were calculated. SUV_{max} differences between benign and malignant lesions were compared, and SUV_{max} differences between low-risk and moderate- to high-risk lesions were compared based on risk stratification. Binary logistic regression was used to draw receiver operating characteristic (ROC) curves of bpMRI, PET/CT, and bpMRI/PET, and the area under the curve (AUC) was

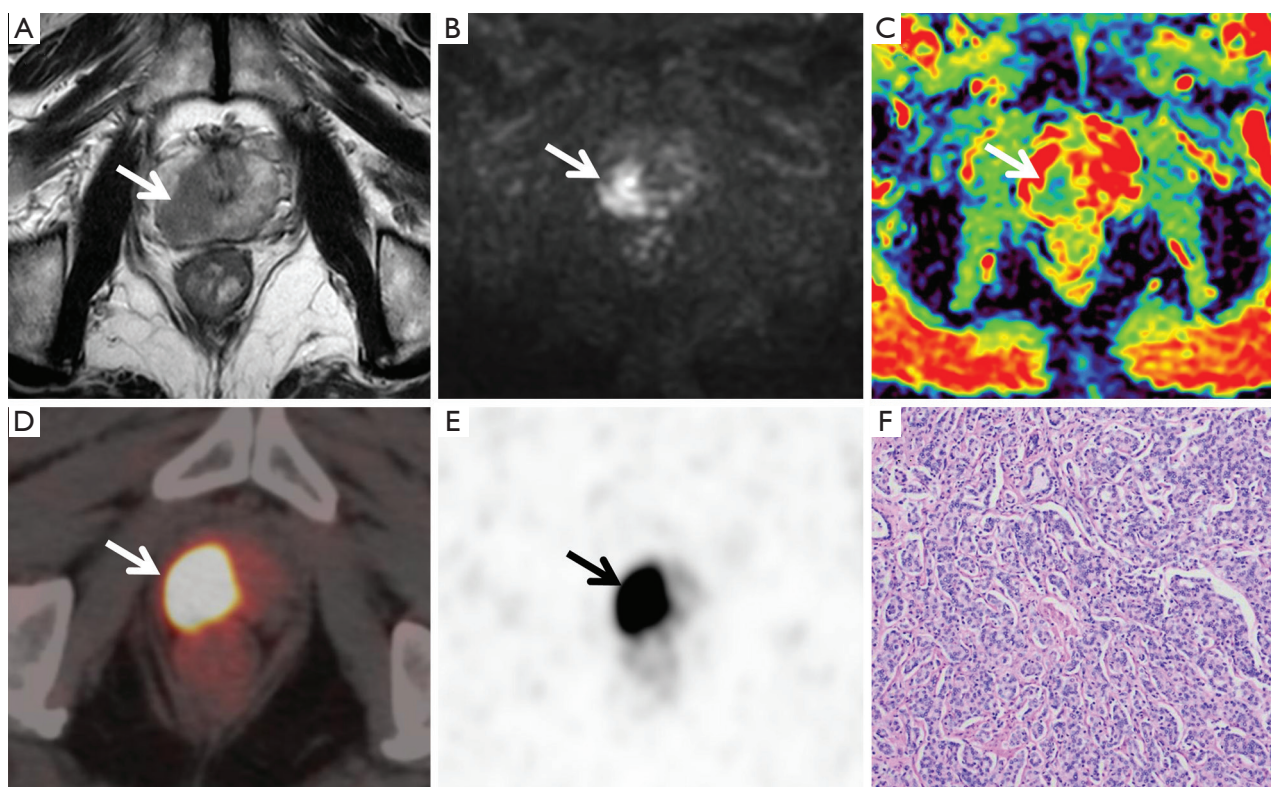


Figure 2 A 72-year-old patient with increased prostate-specific antigen (PSA) on physical examination (PI-RADS =5, SUV_{max} =62.4, Gleason score 4+4 =8, PSA: 31 ng/mL). The signal in the right lobe of the prostate decreased unevenly on T2-weighted imaging (T2WI) (A, arrow), a higher signal was observed on diffusion-weighted imaging (DWI) (B, arrow), and a lower signal was noted on the apparent diffusion coefficient (ADC) map (C, arrow). Obvious radioactive uptake was depicted on positron emission tomography/computed tomography (PET/CT) (arrows in D and E). Prostate cancer was proven by pathology (haematoxylin and eosin staining, $\times 100$; F).

calculated. Pearson correlation analysis was performed on the data fitting a binary normal distribution, and Spearman correlation analysis was performed on ranked data or data with an unknown distribution. All analyses were performed using SPSS (version 19.0, IBM, Armonk, New York) and MedCalc (version 11.5.0, MedCalc) statistical software. $P < 0.05$ was considered statistically significant.

Results

Anatomical locations and lesion identification were consistent between the two radiologists specialising in MRI (95%; Cohen's $\kappa = 0.86$). Of the 105 patients, 68 were diagnosed with PCa (Figure 2), and 37 patients were diagnosed with BPH (Figure 3) with or without prostatitis (Figure 4). The statistical results for the SUV_{max} are shown in Table 2. The SUV_{max} of PCa was significantly higher than that of benign lesions, and the SUV_{max} of moderate-

to high-risk PCa was significantly higher than that of low-risk PCa. The SUV_{max} of benign lesions was significantly lower than that of low-risk PCa. The PI-RADS scores for benign and malignant lesions are shown in Table 3. Of the 68 patients with PCa, 19 underwent radical prostatectomy, including 13 with EPE, eight with SVI, and nine with PLNM. The diagnostic details are shown in Table 4.

The PI-RADS classification was used for MRI diagnosis. The ROC analysis results (Figure 5) showed that a PI-RADS score ≥ 3 can be used as the diagnostic threshold. The accuracy of bpMRI in identifying benign and malignant prostate lesions was similar to that of PET/CT ($SUV_{max} \geq 10.9$). The Youden indices of bpMRI and PET/CT were 0.60 and 0.64 (Table 5), respectively, and the AUCs of bpMRI and PET/CT were 0.87 [95% confidence interval (CI): 0.81–0.94] and 0.85 (95% CI: 0.78–0.92), respectively. With an SUV_{max} greater than 12.9 as the diagnostic threshold (Figure 6), the accuracy of PET/

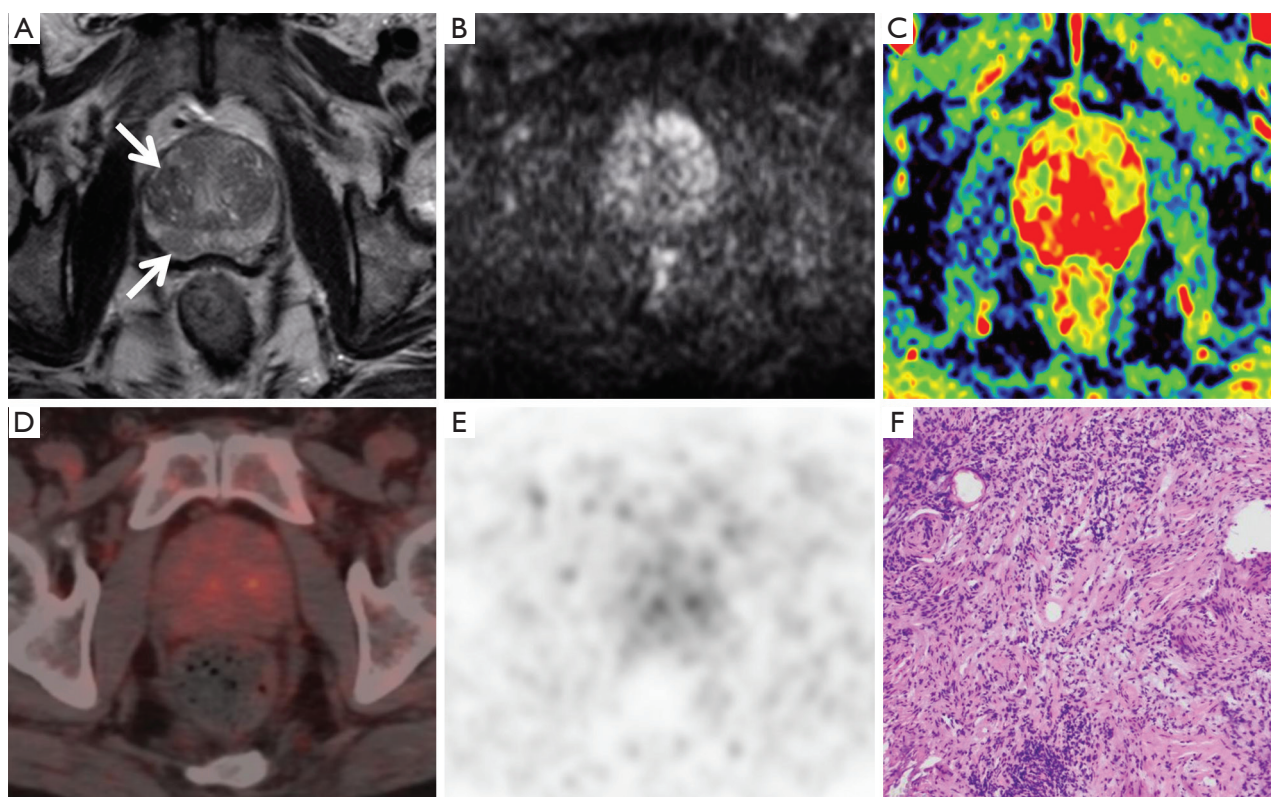


Figure 3 A 65-year-old patient with progressive dysuria for more than one year (PI-RADS =3, PSA: 6.66 ng/mL). On T2-weighted imaging (T2WI), low signals with clear or unclear borders were evident in the peripheral and central gland zones of the prostate (A, arrows). Uneven slightly high signals on diffusion-weighted imaging (DWI) (B) and low signals on the apparent diffusion coefficient (ADC) map (C) were observed in the central gland zone. No obvious radioactive uptake was observed on positron emission tomography/computed tomography (PET/CT) images (D and E). Benign prostatic hyperplasia with prostatitis was confirmed by pathology (haematoxylin and eosin staining, 100× magnification; F).

CT in the differential diagnosis of intermediate- to high-risk PCa versus low-risk PCa or benign lesions was higher than that of bpMRI (PI-RADS score ≥ 4). The Youden indices were 0.68 and 0.51, respectively (Table 5), and the AUCs were 0.88 (95% CI: 0.81–0.95) and 0.83 (95% CI: 0.75–0.90). In patients with PCa, the PI-RADS score and SUV_{max} were positively correlated with the GS ($r=0.386$, $P=0.001$; $r=0.473$, $P=0.000$). The SUV_{max} of PCa lesions was positively correlated with the PI-RADS score ($r=0.616$, $P=0.000$).

The sensitivity and specificity of bpMRI/PET in diagnosing PCa were 94% and 81%, and the AUC and Youden index were 0.90 (95% CI: 0.84–0.96) and 0.75, respectively. The AUC and Youden index values were higher than those of bpMRI or PET/CT alone (Table 5). The sensitivity and specificity of bpMRI/PET in the differential diagnosis of intermediate- to high-risk PCa

versus low-risk PCa or benign lesions were 80% and 88%, respectively, and the AUC and Youden index were 0.90 (95% CI: 0.84–0.95) and 0.68, respectively. The AUC of bpMRI/PET was higher than that of bpMRI or PET/CT alone, and its Youden index was higher than that of bpMRI alone and equal to that of PET/CT alone (Table 5).

Discussion

Due to the excellent tissue contrast and image resolution of MRI, it is the best technique to detect PCa. To date, many types of magnetic resonance sequences are available for prostate examination. Among them, magnetic resonance spectroscopy and DCEI technology are relatively early modalities with their own value. However, their functions have gradually been replaced by DWI technology in the past two decades. We carried out mpMRI studies, including

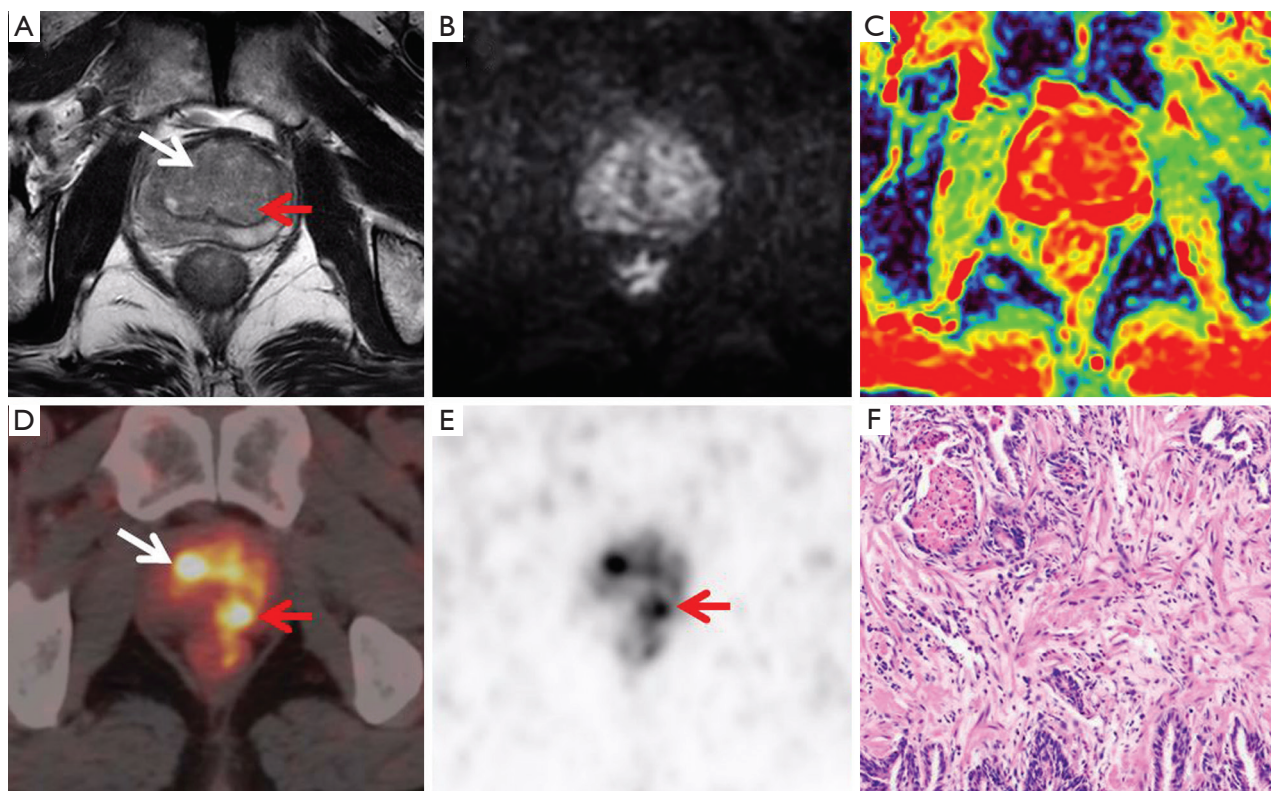


Figure 4 A 67-year-old patient with increased prostate-specific antigen (PSA) (PI-RADS =2, SUV_{max} =12.73, PSA: 5.36 ng/mL). A slightly lower signal with blurred borders was visible in the central gland and right peripheral zone on T2-weighted imaging (T2WI) (A, arrows). The diffusion-weighted imaging (DWI) and apparent diffusion coefficient (ADC) maps did not show abnormal signals (B and C). Positron emission tomography/computed tomography (PET/CT) images revealed obvious uptake of diffuse uneven radioactivity (D and E, arrows). Benign prostatic hyperplasia with prostatitis was confirmed by pathology (haematoxylin and eosin staining, 100x magnification; F).

Table 2 PET/CT quantitative analysis statistics (n=105)

Characteristics [n]	SUV_{max}	P
PCa [68]	15.25 (7.76, 25.36)	0.000 ^a
BL [37]	5.73 (4.41, 8.96)	0.007 ^b
GS=6 [14]	7.02 (4.68, 11.84)	0.014 ^c
GS≥7 [54]	18.89 (12.03, 29.11)	–

^a, BL vs. PCa (all); ^b, BL vs. PCa (GS=6); ^c, PCa (GS=6) vs. PCa (GS≥7). PET/CT, positron emission tomography/computed tomography; BL, benign lesions; PCa, prostate cancer; GS, Gleason score.

Table 3 PI-RADS score results for benign and malignant lesions

PI-RADS	BL (n)	PCa (n)
1	11	0
2	19	14
3	5	16
4	2	20
5	0	18

PI-RADS, prostate imaging-reporting and data system; BL, benign lesions; PCa, prostate cancer.

magnetic resonance spectroscopy and DCEI, in the early stage of this study. The length of each examination was approximately 50 min. A few patients could not tolerate lying on the examination table for such a long time or had to interrupt the examination to urinate. With the

accumulation of research data, researchers in the prostate MRI field have gradually realized that simpler sequence combinations for bpMRI (T2WI + DWI) are also effective. In the recent literature, the diagnostic efficacy of bpMRI has been preliminarily verified. A study by van der Leest

Table 4 Statistics of the results of the invasion of surrounding organizations

Parameters	bpMRI		PET/CT	
	n	%	n	%
EPE	12	92 (12/13)	10	77 (10/13)
SVI	8	100 (8/8)	6	75 (6/8)
PLNM	7	78 (7/9)	9	100 (9/9)

EPE, extraprostatic extension; SVI, invasion of seminal vesicle; PLNM, pelvic lymph node metastasis; PET/CT, positron emission tomography/computed tomography.

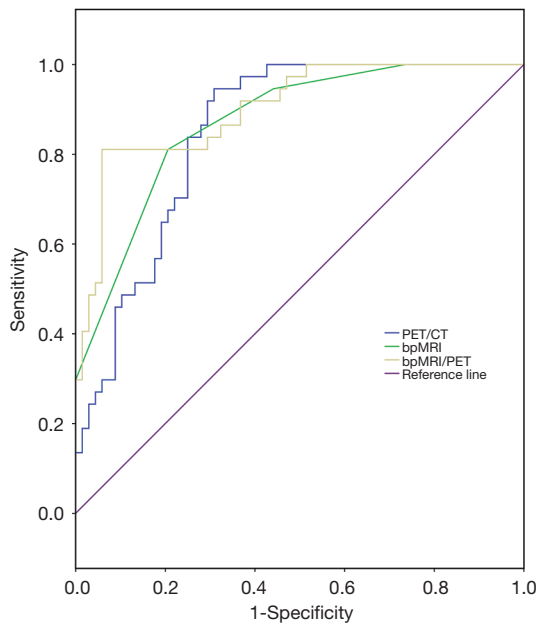


Figure 5 Receiver operating characteristic curve (ROC) analysis of the qualitative diagnosis of prostate cancer.

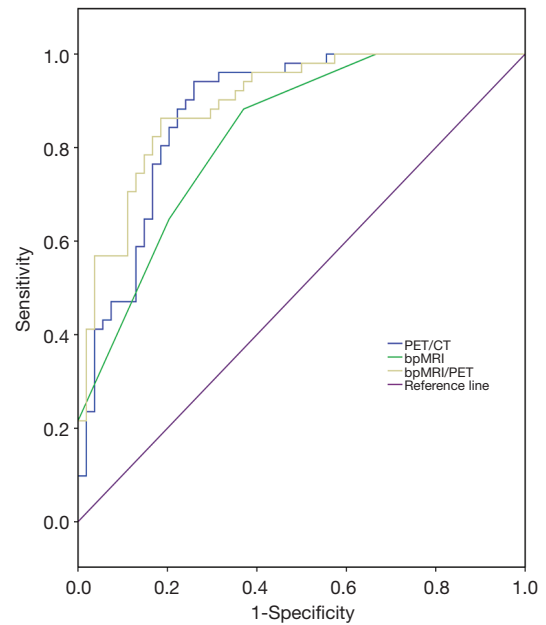


Figure 6 Receiver operating characteristic curve (ROC) analysis of the risk-stratified diagnosis of prostate cancer.

Table 5 Analysis of diagnostic efficacy of bpMRI and PET/CT

Variable	Qualitative diagnosis				Risk stratified diagnosis			
	AUC (95% CI)	Cut-off value	Sensitivity/specificity	Youden index	AUC (95% CI)	Cut-off value	Sensitivity/specificity	Youden index
bpMRI	0.87 (0.79–0.93)	3	0.79/0.81	0.60	0.83 (0.74–0.89)	4	0.63/0.88	0.51
PET/CT	0.85 (0.77–0.91)	10.9	0.69/0.95	0.64	0.88 (0.80–0.93)	12.9	0.74/0.94	0.68
bpMRI/PET	0.90 (0.84–0.96)	NA	0.94/0.81	0.75	0.90 (0.84–0.95)	NA	0.80/0.88	0.68

bpMRI, biparametric magnetic resonance imaging; PET/CT, positron emission tomography/computed tomography; AUC, area under the curve.

et al. showed that bpMRI and mpMRI are equal in both sensitivity (95%) and specificity (69%) (9). The accuracy degree is 0.64, which is similar to the accuracy degree in our study (0.60). BpMRI is a fast, cost-effective, highly accurate noninvasive technique without side effects from contrast injection. Patients may more readily accept this type of examination, which can benefit patients who do not have health insurance or patients in poor countries.

In MRI DWI, PCa is depicted as a change in high-intensity signals. As the b value increases, the contrast between cancerous lesions and benign tissues becomes more obvious. Recognition of this obvious difference depends on the experience of radiologists and cannot be objectively evaluated. The ADC map derived from DWI can be used for quantitative measurement. As the malignancy degree of a lesion increases, the ADC value gradually decreases. Lesions with an SUV_{max} below the diagnostic threshold can be considered suspected PCa. However, this threshold may vary with the machine type and parameter settings and needs to be set according to the specific situation of each hospital. On the ADC map, the signals of cancerous lesions were significantly reduced, with significantly lower ADC values. Benign lesions, including inflammation and hyperplasia, are depicted as slightly reduced signals on ADC map, and their ADC values are higher than that of PCa. The false-positive rate is as high as 60–80% in lesions with PI-RADS scores >4 on mpMRI (17,18). As diagnostic tests, bpMRI, and mpMRI are similar, the false-positive and false-negative rates are still relatively high, and the diagnostic accuracy requires further improvement.

The prognosis of patients with low-risk localized PCa does not significantly differ between treatment options. However, the prognosis of patients with high-risk PCa is better in those undergoing radical prostatectomy. Preoperative risk stratification is conducive to determining the best treatment option for patients. The current study showed that a greater SUV_{max} was associated with a higher GS for a lesion. The SUV_{max} can predict the risk stratification of low-risk patients (GS =6) and moderate- to high-risk patients (GS \geq 7) and has an effect that cannot be ignored when formulating and adjusting treatment plans for patients. This conclusion is similar to that reported in the literature (19,20). Although the mean SUV_{max} of low-risk lesions was lower than that of moderate- to high-risk lesions, it was still significantly higher than that of benign lesions. ROC analysis showed that PET/CT (Youden =0.68) was a more accurate technique for differentiating intermediate- to high-risk PCa from low-risk PCa and benign lesions

than bpMRI (Youden =0.51) and was a more reliable source for preoperative risk stratification of PCa patients. In a study by Lopci *et al.*, when an SUV_{max} greater than 4.8 was set as the diagnostic threshold, PET/CT had a sensitivity and specificity of 82.4% and 72.2%, respectively, in differentiating benign from malignant prostate lesions (21). When an SUV_{max} greater than 5.4 was set as the diagnostic threshold, the sensitivity and specificity of PET/CT in differentiating moderate- to high-risk PCa from low-risk or benign lesions were 100% and 76%, respectively (21). In the current study, the diagnostic threshold set in this study was higher than that in the literature; thus, the diagnostic sensitivity in this study was low, and the diagnosis of some PCa patients with low PSMA expression levels may have been easy to miss. However, the diagnostic specificity was significantly increased in this study. The reasons for the high diagnostic threshold in this study may include racial differences, drug and machine differences, and sampling errors. Although absolute SUV measurements might differ from one institution to another due to applied technical differences when proper quality measures are followed, they are consistent within a given institution. Similarly, although the absolute SUVs of a lesion might differ between PET/CT and PET/MRI measurements and are usually slightly lower in PET/MRI measurements, such measurements are reproducible and consistent. A study by Civelek *et al.* showed that the persistent absolute PET/MRI-derived SUV difference in the liver compared to PET/CT likely originates from hardware and post-processing software differences in the PET/MRI and PET/CT equipment. Although the PET/CT-derived ^{18}F -FDG liver SUV_{max} tended to be slightly higher, no statistically significant difference in the PET/CT-derived ^{18}F -FDG liver SUV_{mean} was noted among the groups. No statistically significant differences in the PET/MRI-derived ^{18}F -FDG liver SUV_{max} and SUV_{mean} were observed among the three groups (22). Overall, we believe that the diagnostic thresholds of different hospitals are not comparable. Provided that verification by pathological study and statistical analysis is performed, the threshold for PCa diagnosis can be set at the reference for the individual hospital. Low radiation uptake on PET/CT was observed in 21 patients whose SUV_{max} was higher than the diagnostic threshold that we set in this study, suggesting the possibility of benign lesions in these patients. However, their pathological results indicated a diagnosis of PCa. The reason may be that higher PSMA expression is present in most PCa lesions, but low PSMA expression may be present in 10% of PCa lesions, which

results in low radiation uptake (12,13).

The diagnostic score for bpMRI is categorical, the results of bpMRI/PET are qualitative, and neither is a continuous quantitative variable. Although the ROC curve was plotted using logistic regression in this study, no high application value was identified to compare AUCs. The Youden index was more appropriate for comparisons of the results in this study. The two imaging methods were assessed by parallel testing. When one of the diagnostic results of bpMRI or PET/CT was positive, the patient was diagnosed with PCa, and when both imaging methods were negative, the patient was diagnosed with non-PCa. In this study, the sensitivity and specificity of bpMRI/PET in diagnosing PCa were 94% and 81%, respectively, and the Youden index was 0.75. The diagnostic sensitivity of bpMRI/PET was significantly higher, the rate of missed diagnosis was lower, and the Youden index was higher than that of MRI or PET/CT examination, which improved the overall ability to differentiate true PCa from non-PCa. In this study, false-positive lesions were shown on bpMRI in seven patients who actually had benign nodular hyperplasia accompanied by prostate inflammation, and these patients were misdiagnosed with PCa based on the PI-RADS score. Among them, positive lesions according to bpMRI were corrected to negative after PET/CT examination in five patients. False-positive results in the peripheral zone are caused by acute and chronic inflammation and fibrosis, which result in low T2WI signal changes or disappearance of the capsule. False-positive results in the central glandular region are mainly due to the similarity of proliferative nodules with matrix components and malignant lesions, which appear as a low signal on T2WI. This study shows that the accuracy of bpMRI/PET is higher than that of bpMRI in predicting PCa risk stratification but similar to that of PET/CT alone. These findings indicate that the combination of the two methods does not improve the accuracy of predicting PCa risk stratification.

A study by Yilmaz *et al.* showed that mpMRI is more accurate in detecting EPE and SVI than PET/CT, while PET/CT is more accurate in detecting lymph node metastasis than mpMRI (23). MpMRI is the preferred method for determining SVI and EPE. For all 19 patients undergoing radical prostatectomy in this study, all SVI cases were identified by bpMRI, and all PLNM cases were identified by PET/CT. The detection rate of EPE by bpMRI was higher than that by PET/CT (92%/77%). The results of this study are similar to those reported in the literature (23). Although PET/CT imaging is slightly more

expensive, it has an irreplaceable role and can be used as a supplementary examination when the diagnosis by bpMRI is not clear. If the SUV_{max} of a patient exceeded 10.9, the specificity of the diagnosis in this study was 95%. Previous studies showed that PET/CT test results could indicate the malignancy of a tumour and had advantages over MRI results in detecting extrapelvic metastases and early recurrence of PCa (13,24,25). Maurer *et al.* confirmed that PET/CT is more accurate than conventional imaging in detecting PCa lymph node metastases and is conducive to providing targeted guidance for extended lymphadenectomy in patients with intermediate- and high-risk PCa (26). Therefore, for patients with suspected PCa and with PI-RADS scores greater than 3 on bpMRI examination, PET/CT can be used for further qualitative diagnosis and to detect systemic lymph nodes and bone metastases, which can be conducive to accurate staging of PCa.

After ultrasound or PSA screening, we recommend MRI and biopsy. MRI is relatively inexpensive and easy to perform. MRI can provide a more accurate diagnosis of benign and malignant lesions, determine whether malignant lesions have EPE and SVI, and enable accurate T staging. Biopsy can exclude false-positive cases on ultrasound and MRI, score malignant lesions, and predict prognosis. Regular PSA screening is recommended for benign cases diagnosed by MRI. For patients with an ambiguous MRI diagnosis who are reluctant to undergo biopsy, we recommend noninvasive ^{68}Ga -PSMA-11 PET/CT to establish a definitive diagnosis. If cancer has been confirmed by MRI or biopsy, ^{68}Ga -PSMA-11 PET/CT examination are necessary to determine the complete staging of the tumour before selecting the optimum treatment plan.

The limitation of this study is that the pathological results were acquired from ultrasound-guided systemic puncture biopsy samples, and no point-to-point analysis of the whole specimen was performed after radical surgery, which may have led to bias in the results. However, we believe that the overall results of this study are still reliable and valuable. Another limitation in this study is that bpMRI and PET/CT were performed separately. For radiologists, suspected lesions are easier to identify on PET/MRI. A lesion may be missed on mpMRI, and reading bpMRI and PET/CT images increases radiologists' workload. Moreover, undergoing two imaging examinations increases patients' costs. A study by Hicks *et al.* showed that PET/MRI had better sensitivity than mpMRI for PCa detection, while the specificity was similar. Additionally, a tumour grade greater than 6.9 suggests a GS of 7 or higher. PET/

MRI has higher accuracy for localizing intraprostatic disease than PET and mpMRI alone. Therefore, clinically significant PCa can be identified, and patients can receive appropriate management (27,28).

Conclusions

The combined application of bpMRI and PET improved the accuracy of the qualitative diagnosis of prostate lesions, and its diagnostic efficacy for risk stratification in patients with intermediate- to high-risk PCa was similar to that of PET/CT and higher than that of bpMRI alone. ⁶⁸Ga-PSMA-11 PET/CT are helpful for staging PCa.

Acknowledgments

Funding: None.

Footnote

Conflicts of Interest: All authors have completed the ICMJE uniform disclosure form (available at <https://dx.doi.org/10.21037/qims-21-80>). The authors have no conflicts of interest to declare.

Ethical Statement: The authors are accountable for all aspects of the work in ensuring that questions related to the accuracy or integrity of any part of the work are appropriately investigated and resolved. The study was conducted in accordance with the Declaration of Helsinki (as revised in 2013). The study was approved by ethics board of KY20171208-03 and individual consent for this retrospective analysis was waived.

Open Access Statement: This is an Open Access article distributed in accordance with the Creative Commons Attribution-NonCommercial-NoDerivs 4.0 International License (CC BY-NC-ND 4.0), which permits the non-commercial replication and distribution of the article with the strict proviso that no changes or edits are made and the original work is properly cited (including links to both the formal publication through the relevant DOI and the license). See: <https://creativecommons.org/licenses/by-nc-nd/4.0/>.

References

1. Siegel RL, Miller KD, Jemal A. Cancer statistics, 2019. *CA Cancer J Clin* 2019;69:7-34.
2. Kasivisvanathan V, Rannikko AS, Borghi M, Panebianco V, Mynderse LA, Vaarala MH, et al. MRI-Targeted or Standard Biopsy for Prostate-Cancer Diagnosis. *N Engl J Med* 2018;378:1767-77.
3. Siddiqui MM, Rais-Bahrami S, Turkbey B, George AK, Rothwax J, Shakir N, Okoro C, Raskolnikov D, Parnes HL, Linehan WM, Merino MJ, Simon RM, Choyke PL, Wood BJ, Pinto PA. Comparison of MR/ultrasound fusion-guided biopsy with ultrasound-guided biopsy for the diagnosis of prostate cancer. *JAMA* 2015;313:390-7.
4. Barbieri S, Brönnimann M, Boxler S, Vermathen P, Thoeny HC. Differentiation of prostate cancer lesions with high and with low Gleason score by diffusion-weighted MRI. *Eur Radiol* 2017;27:1547-55.
5. Bjurlin MA, Meng X, Le Nobin J, Wysock JS, Lepor H, Rosenkrantz AB, Taneja SS. Optimization of prostate biopsy: the role of magnetic resonance imaging targeted biopsy in detection, localization and risk assessment. *J Urol* 2014;192:648-58.
6. Feng ZY, Wang L, Min XD, Wang SG, Wang GP, Cai J. Prostate Cancer Detection with Multiparametric Magnetic Resonance Imaging: Prostate Imaging Reporting and Data System Version 1 versus Version 2. *Chin Med J (Engl)* 2016;129:2451-9.
7. Li M, Chen T, Zhao W, Wei C, Li X, Duan S, Ji L, Lu Z, Shen J. Radiomics prediction model for the improved diagnosis of clinically significant prostate cancer on biparametric MRI. *Quant Imaging Med Surg* 2020;10:368-79.
8. Kang Z, Min X, Weinreb J, Li Q, Feng Z, Wang L. Abbreviated Biparametric Versus Standard Multiparametric MRI for Diagnosis of Prostate Cancer: A Systematic Review and Meta-Analysis. *AJR Am J Roentgenol* 2019;212:357-65.
9. van der Leest M, Israël B, Cornel EB, Zámečník P, Schoots IG, van der Lelij H, Padhani AR, Rovers M, van Oort I, Sedelaar M, Hulsbergen-van de Kaa C, Hannink G, Veltman J, Barentsz J. High Diagnostic Performance of Short Magnetic Resonance Imaging Protocols for Prostate Cancer Detection in Biopsy-naïve Men: The Next Step in Magnetic Resonance Imaging Accessibility. *Eur Urol* 2019;76:574-81.
10. Alabousi M, Salameh JP, Gusenbauer K, Samoïlov L, Jafri A, Yu H, Alabousi A. Biparametric vs multiparametric prostate magnetic resonance imaging for the detection of prostate cancer in treatment-naïve patients: a diagnostic test accuracy systematic review and meta-analysis. *BJU Int*

- 2019;124:209-20.
11. Afshar-Oromieh A, Malcher A, Eder M, Eisenhut M, Linhart HG, Hadaschik BA, Holland-Letz T, Giesel FL, Kratochwil C, Haufe S, Haberkorn U, Zechmann CM. PET imaging with a [68Ga]gallium-labelled PSMA ligand for the diagnosis of prostate cancer: biodistribution in humans and first evaluation of tumour lesions. *Eur J Nucl Med Mol Imaging* 2013;40: 486-95.
 12. Bostwick DG, Pacelli A, Blute M, Roche P, Murphy GP. Prostate specific membrane antigen expression in prostatic intraepithelial neoplasia and adenocarcinoma: a study of 184 cases. *Cancer* 1998;82:2256-61.
 13. Maurer T, Eiber M, Schwaiger M, Gschwend JE. Current use of PSMA-PET in prostate cancer management. *Nat Rev Urol* 2016;13:226-35.
 14. Domachevsky L, Goldberg N, Gorenberg M, Bernstine H, Groshar D, Catalano OA. Prostate cancer evaluation using PET quantification in 68Ga-PSMA-11 PET/MR with attenuation correction of bones as a fifth compartment. *Quant Imaging Med Surg* 2020;10:40-7.
 15. Freitag MT, Radtke JP, Afshar-Oromieh A, Roethke MC, Hadaschik BA, Gleave M, Bonekamp D, Kopka K, Eder M, Heusser T, Kachelriess M, Wiczorek K, Sachpekidis C, Flechsig P, Giesel F, Hohenfellner M, Haberkorn U, Schlemmer HP, Dimitrakopoulou-Strauss A. Local recurrence of prostate cancer after radical prostatectomy is at risk to be missed in (68)Ga-PSMA-11-PET of PET/CT and PET/MRI: comparison with mpMRI integrated in simultaneous PET/MRI. *Eur J Nucl Med Mol Imaging* 2017;44:776-87.
 16. D'Amico AV, Whittington R, Kaplan I, Beard C, Schultz D, Malkowicz SB, Wein A, Tomaszewski JE, Coleman CN. Calculated prostate carcinoma volume: The optimal predictor of 3-year prostate specific antigen (PSA) failure free survival after surgery or radiation therapy of patients with pretreatment PSA levels of 4-20 nanograms per milliliter. *Cancer* 1998;82:334-41.
 17. Ahmed HU, El-Shater Bosaily A, Brown LC, Gabe R, Kaplan R, Parmar MK, Collaco-Moraes Y, Ward K, Hindley RG, Freeman A, Kirkham AP, Oldroyd R, Parker C, Emberton M; PROMIS study group. Diagnostic accuracy of multi-parametric MRI and TRUS biopsy in prostate cancer (PROMIS): a paired validating confirmatory study. *Lancet* 2017;389:815-22.
 18. Mehralivand S, Bednarova S, Shih JH, Mertan FV, Gaur S, Merino MJ, Wood BJ, Pinto PA, Choyke PL, Turkbey B. Prospective Evaluation of PI-RADS Version 2 Using the International Society of Urological Pathology Prostate Cancer Grade Group System. *J Urol* 2017;198:583-90.
 19. Ferraro DA, Garcia Schüler HI, Muehlematter UJ, Eberli D, Müller J, Müller A, Gablinger R, Kranzbühler H, Omlin A, Kaufmann PA, Hermanns T, Burger IA. Impact of (68)Ga-PSMA-11 PET staging on clinical decision-making in patients with intermediate or high-risk prostate cancer. *Eur J Nucl Med Mol Imaging* 2020;47:652-64.
 20. Chen M, Zhang Q, Zhang C, Zhao X, Marra G, Gao J, Lv X, Zhang B, Fu Y, Wang F, Qiu X, Guo H. Combination of (68)Ga-PSMA PET/CT and Multiparametric MRI Improves the Detection of Clinically Significant Prostate Cancer: A Lesion-by-Lesion Analysis. *J Nucl Med* 2019;60:944-9.
 21. Lopci E, Saita A, Lazzeri M, Lughezzani G, Colombo P, Buffi NM, et al. 68Ga-PSMA Positron Emission Tomography/Computerized Tomography for Primary Diagnosis of Prostate Cancer in Men with Contraindications to or Negative Multiparametric Magnetic Resonance Imaging: A Prospective Observational Study. *J Urol* 2018;200:95-103.
 22. Civelek AC, Rana A, Malayeri AA, Rodante J, Mehta NN, Bluemke DA. PET-MRI derived 18F-FDG liver SUV metrics: effects of Hepatic Steatosis and comparison with PET-CT. *J Nucl Med* 2017;58:455.
 23. Yilmaz B, Turkay R, Colakoglu Y, Baytekin HF, Ergul N, Sahin S, Tugcu V, Inci E, Tasci AI, Cermik TF. Comparison of preoperative locoregional Ga-68 PSMA-11 PET-CT and mp-MRI results with postoperative histopathology of prostate cancer. *Prostate* 2019;79:1007-17.
 24. Zhang Q, Zang S, Zhang C, Fu Y, Lv X, Zhang Q, Deng Y, Zhang C, Luo R, Zhao X, Wang W, Wang F, Guo H. Comparison of (68)Ga-PSMA-11 PET-CT with mpMRI for preoperative lymph node staging in patients with intermediate to high-risk prostate cancer. *J Transl Med* 2017;15:230.
 25. Calais J, Cao M, Nickols NG. The Utility of PET/CT in the Planning of External Radiation Therapy for Prostate Cancer. *J Nucl Med* 2018;59:557-67.
 26. Maurer T, Gschwend JE, Rauscher I, Souvatzoglou M, Haller B, Weirich G, Wester HJ, Heck M, Kübler H, Beer AJ, Schwaiger M, Eiber M. Diagnostic Efficacy of (68)Gallium-PSMA Positron Emission Tomography Compared to Conventional Imaging for Lymph Node Staging of 130 Consecutive Patients with Intermediate to High Risk Prostate Cancer. *J Urol* 2016;195:1436-43.
 27. Hicks RM, Simko JP, Westphalen AC, Nguyen HG, Greene KL, Zhang L, Carroll PR, Hope TA. Diagnostic

Accuracy of (68)Ga-PSMA-11 PET/MRI Compared with Multiparametric MRI in the Detection of Prostate Cancer. *Radiology* 2018;289:730-7.

28. Civelek AC. (68)Ga-PSMA-11 PET: Better at Detecting Prostate Cancer than Multiparametric MRI? *Radiology* 2018;289:738-9.

Cite this article as: Nuo Y, Li A, Yang L, Xue H, Wang F, Wang L. Efficacy of ⁶⁸Ga-PSMA-11 PET/CT with biparametric MRI in diagnosing prostate cancer and predicting risk stratification: a comparative study. *Quant Imaging Med Surg* 2022;12(1):53-65. doi: 10.21037/qims-21-80